



Investigating the pressure distribution of an airfoil with a cylindrical body

Mohammad Hossein Ghadimi Gorakhk ^{a1}, Malek Ashtar University of Technology, Tehran Province, Tehran, Lavizan, Babaei Hwy., Shabanlou, QFMV+C59, Iran, mohamadhoseinghadimi102@gmail.com, <https://orcid.org/0009-0002-7367-7584>

Abdolamir Bak Khoshnevis ^b, Hakim Sabzevari University, P.O. Box 9617976487, Sabzevar, Iran, Khoshnevis@hsu.ac.ir, <https://orcid.org/0000-0002-6643-5459>

Suggested Citation:

Gorakhk, M. H. G. & Khoshnevis, A. B. (2025). Investigating the pressure distribution of an airfoil with a cylindrical body. *World Journal of Environmental Research*, 15(2), 132-145. <https://doi.org/10.18844/wjer.v15i2.9918>

Received from March 22, 2025; revised from April 25, 2025; accepted from November 29, 2025

Selection and peer review under the responsibility of Prof. Dr. Haluk Soran, Near East University, Cyprus.

©2025 by the authors. Licensee *United World Innovation Research and Publishing Center*, North Nicosia, Cyprus. This article is an open-access article distributed under the terms and conditions of the Creative Commons Attribution (CC BY) license (<https://creativecommons.org/licenses/by/4.0/>).

©iThenticate Similarity Rate: 3%

Abstract

The interaction between airfoils and cylindrical obstacles has attracted significant research due to its relevance for aerodynamic performance and flow control. However, the influence of surface roughness on pressure distribution remains insufficiently explored, representing a notable research gap. This study investigates the effect of cylinder roughness on the pressure distribution of an adjacent airfoil using an experimental airfoil-cylinder model. Roughness was introduced by wrapping sandpaper around a cylinder positioned at multiple distances from the airfoil. Experiments were conducted in a subsonic wind tunnel with a sizable test section, and measurements were taken at two different flow velocities. Pressure coefficient distributions on the upper and lower surfaces of the airfoil were analyzed and compared across all configurations. The results indicate that the presence of cylinder roughness reduces pressure coefficients, with effects diminishing as the cylinder is placed further from the airfoil. These findings demonstrate that both cylinder roughness and its proximity influence aerodynamic interactions, offering insights into flow control strategies and design optimization. The study provides a foundation for further investigations into the manipulation of surface features to enhance aerodynamic performance in engineering applications.

Keywords: Aerodynamic interaction; airfoil-cylinder model; flow control; pressure distribution; surface roughness.

* ADDRESS FOR CORRESPONDENCE: Mohammad Hossein, Ghadimi Gorakhk, Malek Ashtar University of Technology, Tehran Province, Tehran, Lavizan, Babaei Hwy., Shabanlou, QFMV+C59, Iran. *E-mail address:* mohamadhoseinghadimi102@gmail.com

1. INTRODUCTION

In today's technologies, the issue of optimizing systems, energy consumption, production materials, etc., is always discussed. One of these is improving and increasing the efficiency of aircraft by examining their aerodynamics. If we look in more detail, in naval aircraft, which, due to necessity, must operate near ships and always serve in unstable weather conditions or turbulent air flows, it is possible to improve their performance and increase their stability through aerodynamic optimization (Lefebvre & Jones, 2019). In this regard, Lefebvre & Jones (2019) have experimentally investigated the loads applied to an airfoil in the downstream of a cylinder. The airfoil was subjected to different angles of attack ranging from -20 to 20 degrees, and the loads were measured using particle image velocimetry. For the case where X/D equals 2, with D representing the cylinder diameter, the wake behind the cylinder assumes the form of two counter-rotating vortices arranged in a side-by-side configuration, which generates negative drag on the airfoil. When the cylinder airfoil spacing increases to X/D equals 3, the cylinder wake transitions into a von Kármán vortex street that produces an unsteady oscillatory flow field. Recent experimental investigations have further demonstrated that interactions between the cylinder wake and the downstream airfoil alter the aerodynamic force response and associated flow structures, thereby emphasizing the role of vortex shedding and wake modulation in comparable configurations (Wang et al., 2024).

Noise generation by aerodynamic structures, especially airfoils, has always been one of the major challenges in aerospace engineering and other related fields. Tonal noise, which appears as a distinct and dominant frequency, is often caused by vortex phenomena and flow separation. Recent aeroacoustic measurements demonstrate that vortex interference significantly alters tonal noise emission and wake structures in airfoils subject to upstream vortices (Yang et al., 2025). Takagi et al. (2006) investigate the effect of the wake flow of a circular cylinder on the tonal noise and aerodynamic characteristics of a NACA0018 airfoil. Recent work has also shown that the aerodynamic response of airfoils under turbulent and unsteady inflow conditions exhibits significant variation in force and wake structures, indicating complex interactions between flow disturbances and airfoil oscillations (Zhao et al., 2025). The main objective of their research is to understand how the nature of the cylinder wake flow, such as the frequency and intensity of the vortices, changes, and its effect on the noise generation mechanisms and airfoil performance. This study seeks to find solutions to reduce noise and improve airfoil performance using wake flow control. The findings demonstrate that the tonal noise generated by the airfoil is reduced due to the presence of the cylinder wake, and the aerodynamic performance is enhanced relative to the condition in which no cylinder wake is present. It should be emphasized that these measurements were carried out within an acoustic wind tunnel environment.

Hooper and McKeon (2021) conducted a complementary investigation that contrasted the freely responding motion of an airfoil located in the wake of a circular cylinder with a controlled driven motion of an airfoil in an equivalent arrangement. This comparison was enabled through simultaneous acquisition of both the airfoil kinematics and the adjacent flow field. In the passive configuration, the mounting permits transverse heaving movement of the airfoil in reaction to incident unsteady forcing, although this setup introduces considerable parasitic influences on the motion such as friction. The driven configuration was able to replicate the essential features of the non-ideal passive response, thereby supporting the use of an idealized sinusoidal motion as an appropriate model for the dynamics of a passive airfoil functioning within a more practical engineering setting. Subsequently, particle image velocimetry measurements for the driven configuration were employed to clarify the dominant flow structures that contribute to the power

generation and thrust observed in both configurations.

Lefebvre (2021) experimentally studied the effect of changes in free stream velocity on the surface pressure distribution of an airfoil located downstream of a circular cylinder. This study was conducted using wind tunnel experiments. The airfoil was positioned downstream of a circular cylinder. The geometric parameters were kept constant in these experiments to allow the effect of free-stream velocity to be investigated purely. Two different free stream velocities were tested: 25 and 40 m/s. At both speeds, precise measurements of the pressure coefficient (C_p) on the airfoil surface were made. These measurements were made by pressure sensors mounted on the airfoil surface. The results of the experiments showed that changing the free stream velocity from 25 to 40 m/s had a relatively small effect on the airfoil pressure coefficient. This change was less than 5%. The overall pressure patterns and the location of the main suction points on the airfoil surface remained almost unchanged. This finding indicates that under the conditions studied, the main mechanisms of flow formation and pressure distribution, which are mainly influenced by the wake vortices of the cylinder and the airfoil geometry, are less sensitive to the free stream velocity.

Mittal and Balachandar (1995) compare two-dimensional and three-dimensional (3D) simulations of flow around cylinders that appear two-dimensional geometrically but have three-dimensional effects. The main objective is to investigate the effect of three-dimensionality on the lift and drag forces and flow stability, compared to the ideal two-dimensional model. This research uses the numerical simulation method to solve the equations of fluid dynamics (CFD). The results showed that there are significant differences between the 2D and 3D models. In the 2D model, the vortices generated by the cylinder are very regular and have high longitudinal coherence. This regularity leads to strong and predictable oscillations in the forces acting on the cylinder, especially the lift force. The amplitude of the lift force oscillation in the 2D case can be up to 1.5 times greater than in the 3D case. In the 3D model, the presence of the third dimension causes the complete order of the vortices to be lost. Small secondary vortices form near the trailing edge of the cylinder. These phenomena lead to a decrease in the flow coherence in the transverse direction (spanwise coherence). As a result, the amplitude of the pressure oscillations on the cylinder, as well as the oscillations of the lift and drag forces, are significantly reduced (up to about 30%).

Earlier research has demonstrated that the interaction between the wake generated by a cylinder and an airfoil undergoing pitching oscillations can produce notable alterations in aerodynamic behavior. The examination of unsteady aerodynamic phenomena is of considerable significance because of wide-ranging engineering applications, including wind turbines, flow energy harvesting through flapping foil mechanisms, unmanned aerial vehicles, and bio-inspired flight systems. Advances in this domain can enhance the maneuverability of aerial and marine vehicles and support the development of innovative systems for emerging missions. The following section provides a concise survey of relevant contributions. A historical examination of this topic reveals that numerous investigators have analyzed different geometric and flow arrangements and characterized their dynamical features. When a static airfoil maintained at fixed angles of attack is positioned either within the wake of an upstream bluff body or near its trailing boundary, the resulting flow exhibits distinct patterns, and a variety of phenomena may arise, including paired vortex shedding, Karman vortex street formation, shear layer reattachment, flow separation, and vortex impingement (Liao et al., 2004).

Rad & Khoshnevis (2023) specifically focus on the experimental investigation of the flow structure of an airfoil exposed to a cylinder wake flow and simultaneously undergoing pitching oscillation. This research was conducted using wind tunnel experiments and hot-wire anemometry. The Reynolds number ($Re = 10^5$),

which represents the range of relatively turbulent flow. In these experiments, a circular cylinder was placed upstream, and a NACA0012 airfoil capable of pitching oscillation was placed. The findings of this study showed that increasing the amplitude of the airfoil's pitching causes the central turbulent region around the airfoil to expand. This change in the turbulent region, in turn, leads to changes in the pressure distribution on the airfoil surface. In another study, Derakhshandeh et al. (Derakhshandeh et al., 2016) investigated flow-induced vibrations on an airfoil that is elastically mounted and exposed to the wake flow of a cylinder. The geometric and flow conditions that lead to maximum energy extraction from these vibrations are determined through experimental tests. The research was conducted in a water channel to allow for more detailed observation of flow and vibration phenomena. The airfoil used is a NACA0012 and is mounted to have two degrees of freedom: heave and pitching. This means that the airfoil can move up and down as well as rotate around an axis. A circular cylinder is also placed upstream of the airfoil. The experimental results showed that the maximum energy harvesting from airfoil vibrations occurs within a certain range of the airfoil's geometric position relative to the cylinder. The flow images showed that the geometric position of the airfoil directly affects the pattern of vortices that exit the cylinder and impinge on the airfoil. These vortical patterns exert alternating forces on the airfoil and excite vibrations in its elastic state.

In another work, Han et al. (2021) examined the interaction between the pitching oscillation of a NACA0012 airfoil and the flow around a circular cylinder located upstream of the airfoil. The effect of the airfoil oscillation on the separation of vortices from the cylinder and the resulting reduction in drag force, as well as the effect of the distance of the cylinder from the airfoil on this phenomenon, was demonstrated. This research was carried out using a coupled numerical solution of fluid dynamics equations. This method allows modeling of complex interactions between flow and body motion. The modeling was carried out in two dimensions. The investigation showed that a pitching oscillating NACA0012 airfoil is capable of modifying the vortex shedding period. In addition, the configuration can produce a drag reduction rate of up to 50.5 percent, which suggests meaningful potential for practical drag mitigation applications in engineering contexts such as launch vehicle components, ship masts, and submarine pipelines.

The airfoil cylinder configuration has attracted sustained international research interest, and extensive findings have been reported in this area. Although these investigations address a common subject, each study introduces a distinctive aspect that contributes novelty and often involves the assessment of additional measurable parameters. For example, Ghadimi et al. (2025) have evaluated such a topic experimentally and have shown the pressure distribution of the airfoil downstream of the flow of a cylinder. In Lefebvre & Jones (2019), the same review was done, while the diameter of the cylinder is the same as the chord of the airfoil, but in the Ghadimi et al., (2025) study it is observed that the diameter of the cylinder is the same as the maximum thickness of the airfoil, so the cylinder is much smaller and has a different effect. Four different cylinder distances from the airfoil, three different angles of attack, and two free-stream velocities are among the conditions examined in this experiment. Finally, according to the data, it is concluded that in each case of the airfoil, the maximum value of the pressure coefficient increases with increasing angle of attack. Also, this maximum value has moved towards the leading edge at the lower level with increasing angle of attack, while at the upper level, conversely, with increasing angle of attack, the maximum value has moved towards the trailing edge of the airfoil. Antinucci et al. (2023) investigated the effects of multi-suction jets on the NACA0012 airfoil's aerodynamic characteristics at $Re=0.54\times10^5$. Both experimental approaches and numerical simulations have been conducted to address this objective. The airfoil surface is outfitted with several suction slots, and the resulting aerodynamic forces are quantified. The analysis also examines flow reattachment behavior in order to determine the most effective control

configuration. The findings indicate that multiple suction jets placed along the upper surface of the airfoil blade produce the greatest enhancement in the lift coefficient. In particular, the numerical results show that the lift coefficient can increase by as much as 480 percent at a stall angle of attack of 22 degrees and a flow velocity of 8 meters per second when suction slots are utilized.

In marine engineering, propellers play a fundamental role in propelling ships through water and form the core of a vessel's propulsion system. Among these, the Sharow propeller represents a notable advancement in marine propulsion technology, designed to enhance efficiency and reduce fuel consumption. Owing to its distinctive design, the Sharow propeller substantially lowers drag while increasing thrust, thereby improving propulsion efficiency and achieving fuel savings of up to 15 percent compared with conventional propellers (Naderyi et al., 2025). In a related study, Abbaspour et al. (2025) optimized the horizontal spacing between a circular cylinder and a NACA0012 airfoil in a cylinder airfoil configuration at various angles of attack using a multi-objective genetic algorithm. The study aimed to minimize volumetric entropy generation while maximizing aerodynamic efficiency under unsteady flow conditions. Furthermore, the effects of the horizontal cylinder airfoil distance on entropy generation rates arising from viscous and turbulent losses, overall volumetric entropy generation, and aerodynamic efficiency were examined. The findings revealed that at low angles of attack, specifically zero degrees, the viscous losses dominate entropy generation due to strong flow adherence to the airfoil surface. As the angle of attack increases and flow separation occurs, entropy generation due to turbulent losses surpasses that associated with viscous effects. At higher angles of attack, namely ten, fifteen, and twenty degrees, flow separation at the trailing edge of the airfoil plays a significant role in augmenting overall entropy generation.

1.1. Purpose of study

In this study, a cylinder airfoil configuration is employed to investigate the influence of surface roughness on the pressure distribution along the airfoil. The cylinder is circular and is located at four different distances from the airfoil. An industrial sandpaper sheet completely covers the cylinder to create roughness. However, to better understand the effect of roughness, three types of sandpaper with different sizes are used. In addition, a smooth cylinder is also tested. The air flow velocity inside the test section is set at 25 and 40 m/s.

2. METHODS AND MATERIALS

In this section, the study explains the method of obtaining data as an experiment and introduces the setup used.

2.1. Wind tunnel facility

A wind tunnel is a laboratory facility designed to study the behavior of air flow and its effects on various objects. This helps researchers and engineers to examine how objects behave in relation to flow, such as cars, airplanes, buildings, and other structures. Modeling in a wind tunnel is an important process in aerospace engineering, automotive, and other industries related to fluid dynamics. The main goal of this process is to study the behavior of flow and its effects on various objects.

The wind tunnel used in this experiment is a subsonic, open-circuit, suction type, with a test section of 120×110 cm, a maximum speed of 60 m/s, and a fan power of 110 kW. This is one of the existing laboratory facilities of Hakim Sabzevari University, which has long served researchers and researchers interested in this field (Figure 1).

Figure 1

The view of the wind tunnel belongs to Hakim Sabzevari University.



2.2. Measurement technique

The pressure measuring device used in this experiment was a digital manometer with the brand name Testo 510i, manufactured by the Testo company located in Germany, and is one of the best available models in Iran.

2.3. Experiment configuration

In this study, the airfoil considered is of the NACA0012 type with a chord length of $C=30\text{cm}$ and a circular cylinder with a diameter of $D=3\text{cm}$. The airfoil has been tested without an angle of attack. The tested distances for the cylinder from the airfoil are at stations $0.25C$, $0.5C$, $0.75C$, and C , respectively. Sandpaper plates have been used to provide roughness. These plates are placed on the cylinder in each test and act as a roughness for the test. Three types of roughness are included, namely 120, 80, and 60, which are fine, medium, and coarse sizes, respectively. Table 1 shows all the tested cases separately. Figures 2-3 also show the arrangement of the cylinder and the airfoil.

Table 1

The conditions of each of the experiments performed

Exp. No.	V (m/s)	L (cm)	R.	Exp. No.	V (m/s)	L (cm)	R.
1	25	0.25C	0	17	40	0.25C	0
2	25	0.25C	60	18	40	0.25C	60
3	25	0.25C	80	19	40	0.25C	80
4	25	0.25C	120	20	40	0.25C	120
5	25	0.5C	0	21	40	0.5C	0
6	25	0.5C	60	22	40	0.5C	60
7	25	0.5C	80	23	40	0.5C	80
8	25	0.5C	120	24	40	0.5C	120
9	25	0.75C	0	25	40	0.75C	0
10	25	0.75C	60	26	40	0.75C	60
11	25	0.75C	80	27	40	0.75C	80
12	25	0.75C	120	28	40	0.75C	120
13	25	1C	0	29	40	1C	0
14	25	1C	60	30	40	1C	60
15	25	1C	80	31	40	1C	80
16	25	1C	120	32	40	1C	120

Figure 2
Test section dimensions and airfoil-cylinder arrangement

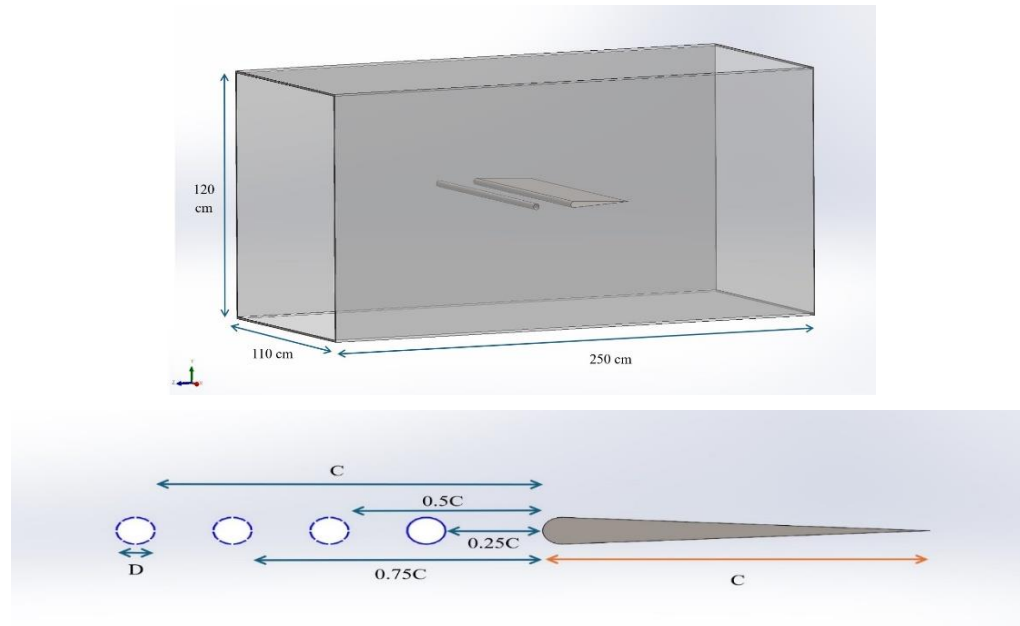


Figure 3
View of the airfoil-cylinder in the wind tunnel



The pressure coefficient relation used in this study is as follows

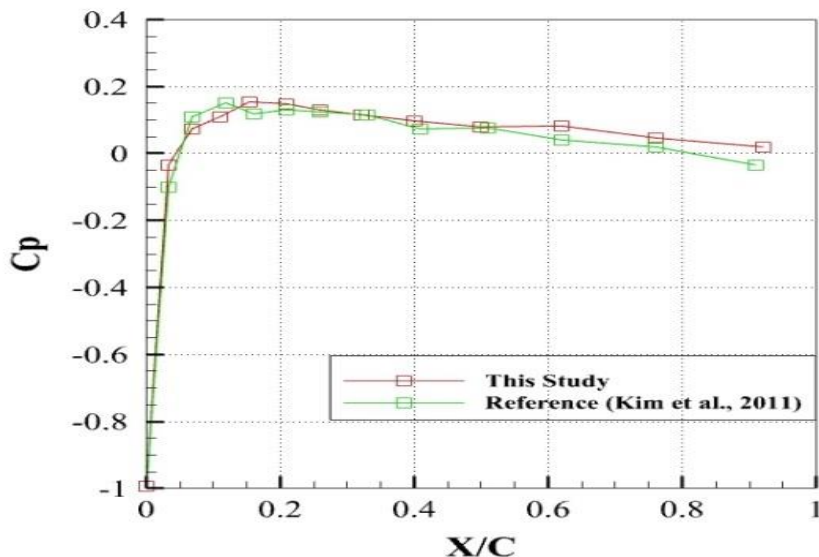
$$C_P = \frac{P - P_\infty}{q_\infty} \quad (1)$$

where P is the static pressure on the airfoil surface, P_∞ is the static pressure inside the test section, and q_∞ is the dynamic pressure inside the test section.

2.4. Validation

The pressure coefficient diagram of the Naca0012 airfoil alone was obtained and compared with reference (Kim et al., 2011). The result shows a very small error, the main reason for which can be stated as the difference in the measurement method, the error of the device, and the operator's reading. Both experiments were carried out with flow conditions $Re=4.8\times10^4$ and under an angle of attack of 1 degree (Figure 4).

Figure 4
 C_p in terms of X/C for a single airfoil



3. RESULTS

This section contains the results and test data. The plots are the pressure coefficient in terms of X/C , which are the points embedded in the upper and lower surfaces of the airfoil. Each plot is shown for the roughness used (4 types, smooth R.0, R.120, R.80, and R.60), distance of the cylinder from the airfoil (4 distances, 0.25C, 0.5C, 0.75, and 1C), and the flow velocity inside the test section (25 and 40 m/s). Figure 5 shows the airfoil pressure coefficient (C_p) at two flow velocities of 25 and 40 m/s for a case where the cylinder is without roughness and is located at a distance of 0.25C from the airfoil. As can be seen, C_p has decreased with increasing flow velocity. The next impression is that at the lower surface of the airfoil, the maximum C_p is applied near the leading edge and at $X=2$. While the maximum pressure is applied at the upper surface at $X=7$. In addition, the convergence of the graphs towards a common point will also indicate the accuracy of the results. By adding roughness No.120 to the cylinder in Figure 6, it is found that the pressure distribution has maintained its overall state, but at the lower level, the maximum pressure is. C_p has increased by 9.4% at both flow velocities. Although this factor has not changed significantly at the upper level.

Figure 8 is the C_p graph for cylinder with No.80 roughness. This reduces the maximum C_p at the upper surface by 22.7% and 21.4% at $V=25$ and 40 m/s, respectively. By increasing the distance of the circular cylinder from the airfoil to $0.5C$ in Figure 9 (without roughness), the pressure distribution becomes more normal, and it can be said that the effect of the cylinder is reduced. Here, the maximum C_p has decreased by 15% and 7.2% at the upper surface and 38.8% and 38% at the lower surface at $V=25$ and 40 m/s, respectively, compared to the test without roughness of $0.25C$ (Figure 5). As mentioned earlier, by applying a roughness No.120 to the cylinder in Figure 10, the values of the four maximum C_p have also decreased. In terms of pressure distribution, in the case of $R.0$ and $R.120$, it is found that the pressure increases from the leading edge and reaches its maximum value approximately at the point $X=5$ and then decreases with a slight slope. Instead, despite the coarser roughness ($R.80$ and $R.60$) in Figures 11 and 12, near the leading edge on both surfaces of the airfoil, there is initially a sharp decrease in the pressure value, and as it progresses towards the leading edge, the pressure increases so that at approximately $X=9$, the maximum C_p is observed.

Comparable trends are observed across the remaining data sets. Overall, increasing the flow velocity in all tests tends to shift the pressure coefficient values toward more positive levels. Additionally, increasing the spacing between the cylinder and the airfoil diminishes the influence of the cylinder, thereby reducing the impact of surface roughness on the observed pressure distribution.

Figure 5
 C_p in terms of $X/C - L=0.25C$ and $R.0$

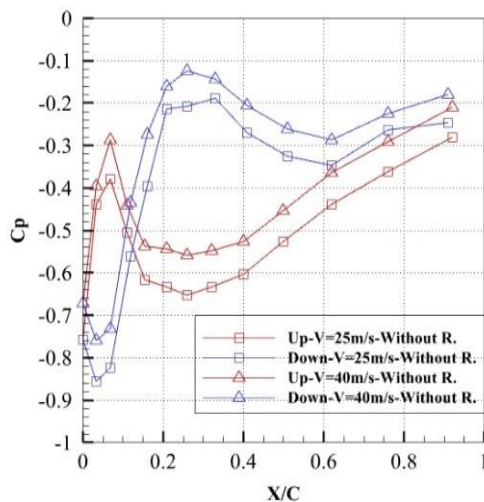


Figure 6
 C_p in terms of $X/C - L=0.25C$ and $R.120$

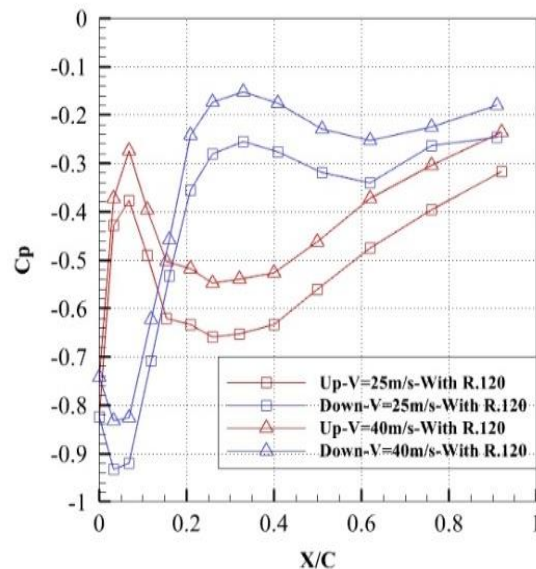


Figure 7
 C_p in terms of $X/C - L=0.25C$ and $R.80$

Figure 8
 C_p in terms of $X/C - L=0.25C$ and $R.60$

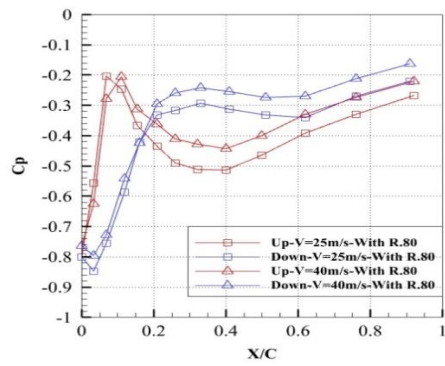


Figure 9
 C_p in terms of $X/C - L=0.5C$ and $R.0$

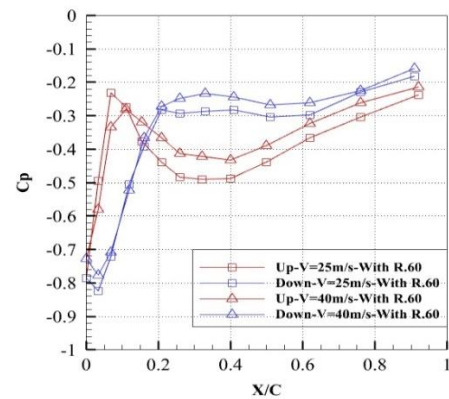


Figure 10
 C_p in terms of $X/C - L=0.5C$ and $R.120$

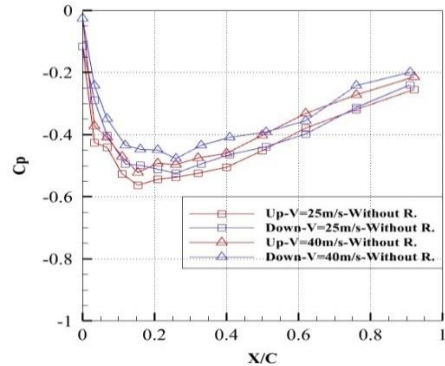


Figure 11
 C_p in terms of $X/C - L=0.5C$ and $R.80$

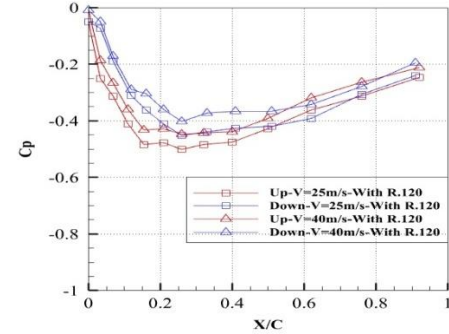


Figure 12
 C_p in terms of $X/C - L=0.5C$ and $R.60$

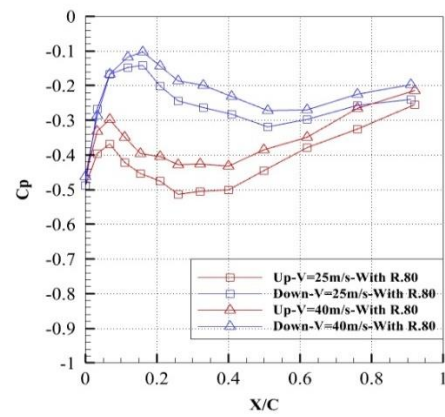


Figure 13
 C_p in terms of $X/C - L=0.75C$ and $R.0$

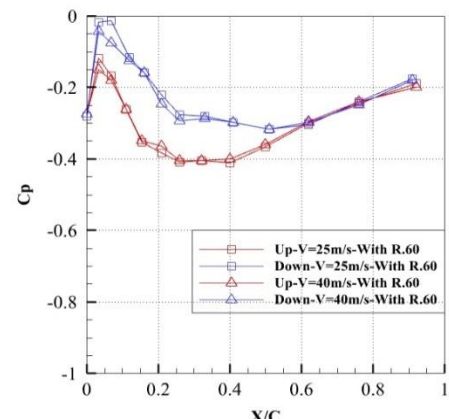


Figure 14
 C_p in terms of $X/C - L=0.75C$ and $R.120$

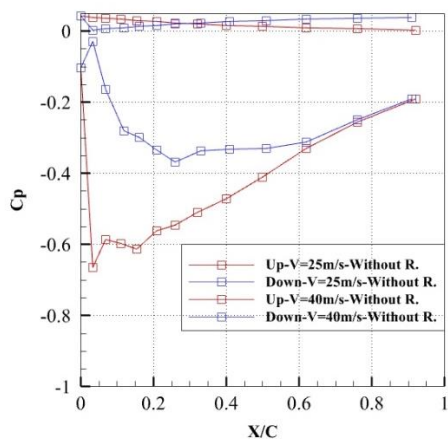


Figure 15
 C_p in terms of $X/C - L=0.75C$ and $R.80$

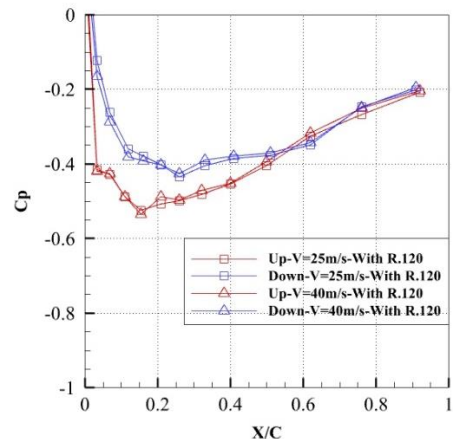


Figure 16
 C_p in terms of $X/C - L=0.75C$ and $R.60$

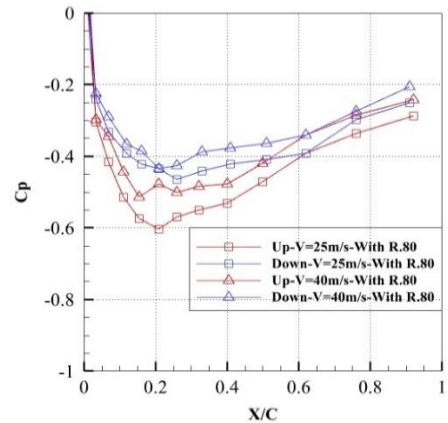


Figure 17
 C_p in terms of $X/C - L=1C$ and $R.0$

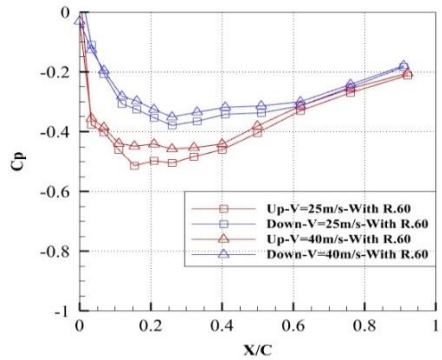


Figure 18
 C_p in terms of $X/C - L=1C$ and $R.120$

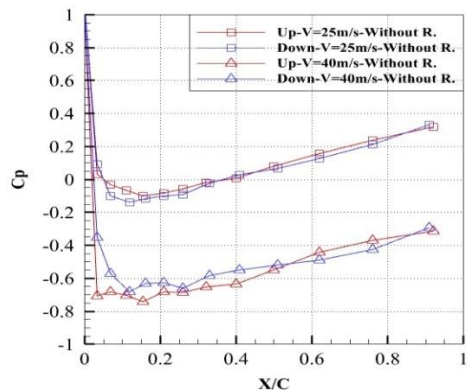


Figure 19
 C_p in terms of $X/C - L=1C$ and $R.80$

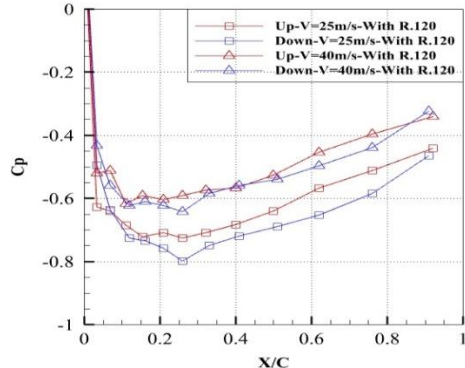
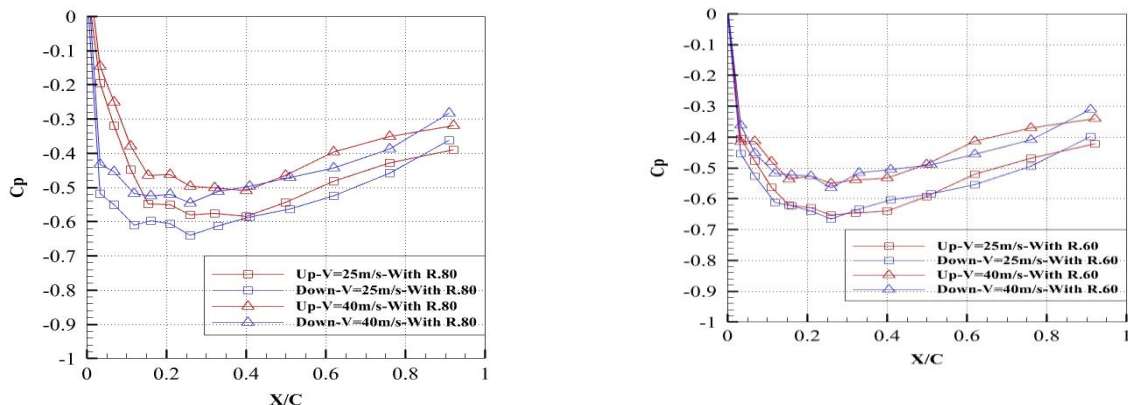


Figure 20
 C_p in terms of $X/C - L=1C$ and $R.60$



4. DISCUSSION

The experimental results demonstrate that the pressure distribution on a NACA0012 airfoil downstream of a cylinder is strongly influenced by both the cylinder-to-airfoil spacing and the surface roughness of the cylinder. When the cylinder is closest to the airfoil (0.25C), the wake effect is strongest, producing higher maximum pressure coefficients on both the upper and lower surfaces. Increasing the distance to 0.5 °C, 0.75 °C, and 1 °C progressively attenuates this influence, consistent with Lefebvre & Jones (2019) and Han et al. (2021), who reported that wake strength diminishes with increasing separation and that closer spacing amplifies vortex–airfoil interactions. Similarly, the present results corroborate Rad & Khoshnevis (2023) and Derakhshandeh et al. (2016), showing that upstream cylinder vortices modify local pressure patterns and can induce changes in force distributions on a downstream pitching or stationary airfoil.

The effect of cylinder roughness in this study introduces additional modifications to the pressure profile. Fine roughness (R120) slightly increases the maximum pressure on the lower surface, while coarser roughness (R80 and R60) causes more pronounced shifts, including an initial drop near the leading edge followed by a delayed maximum near the trailing edge. These observations align with prior studies highlighting the sensitivity of downstream airfoil forces to upstream flow perturbations (Yang et al., 2025; Ghadimi et al., 2025), while extending them by demonstrating that surface roughness significantly modulates the vortex strength and impingement pattern. This indicates that cylinder roughness is a non-negligible parameter in wake–airfoil interaction studies, potentially comparable in impact to changes in angle of attack or free-stream velocity reported by Lefebvre (2021).

The influence of flow velocity in this study appears secondary compared with spacing and roughness, with higher velocities slightly increasing the overall pressure coefficients but preserving the qualitative trends. This corroborates Lefebvre (2021), who observed minimal changes in C_p with free-stream velocity variations, and contrasts with more idealized numerical studies (Mittal & Balachandar, 1995) in which two-dimensional simulations often exaggerate flow sensitivity. Overall, the findings confirm that cylinder proximity and surface roughness dominate the modulation of downstream pressure distribution, highlighting the complex interplay between vortex shedding, wake coherence, and surface conditions, while providing practical guidance for aerodynamic optimization and flow control in engineering applications such as aircraft, propellers, and energy-harvesting airfoils.

5. CONCLUSION

Analysis of the cylinder's influence on airfoil pressure distribution reveals several key observations. Increasing flow velocity consistently reduces the pressure coefficient, C_p , shifting values toward the positive region of the graph. Similarly, increasing the distance between the cylinder and the airfoil diminishes the cylinder's impact, rendering changes caused by surface roughness less pronounced. Convergence of the pressure distribution curves toward a common point further confirms the reliability and accuracy of the results.

In most scenarios, pressure distribution differs between the upper and lower surfaces of the airfoil. Even at zero angle of attack, the turbulent wake generated by the cylinder strikes the airfoil asymmetrically, producing non-uniform effects across the surfaces. This asymmetry highlights the complex interaction between cylinder-induced turbulence and airfoil geometry, demonstrating that the presence of the cylinder affects the two surfaces differently and cannot be considered uniform in its influence.

Conflict of Interest: The authors declare no conflict of interest.

Ethical Approval: The study adheres to the ethical guidelines for conducting research.

Funding: This research received no external funding.

REFERENCES

Abbaspour, R., Yadegari, M., Khoshnevis, A. B., & Hoseinzade, D. (2025). Optimization of horizontal spacing in cylinder-NACA0012 airfoil configuration in the Sharow propeller using entropy generation analysis and multi-objective genetic algorithm. *Journal of Marine Science and Technology*, 30(4), 909-938. <https://link.springer.com/article/10.1007/s00773-025-01097-5>

Antinucci, A., Benini, F., Copetti, C., Galati, G., & Rizi, G. (2023). Anomalies of non-invertible self-duality symmetries: fractionalization and gauging. *arXiv preprint arXiv:2308.11707*. <https://arxiv.org/abs/2308.11707>

Derakhshandeh, J. F., Arjomandi, M., Dally, B., & Cazzolato, B. (2016). Flow-induced vibration of an elastically mounted airfoil under the influence of the wake of a circular cylinder. *Experimental Thermal and Fluid Science*, 74, 58-72. <https://www.sciencedirect.com/science/article/pii/S0894177715003465>

Ghadimi, A., Ghassemi, H., & Ghadimi, P. (2025). Asymmetric foil application for calm water resistance reduction of a trimaran vessel via vertical and oblique struts under different operational speeds within semi-planing and planing regime. *Ships and Offshore Structures*, 1-14. <https://www.tandfonline.com/doi/abs/10.1080/17445302.2025.2497553>

Han, R., Liu, W., Yang, X. L., & Chang, X. H. (2021). Effect of NACA0012 airfoil pitching oscillation on flow past a cylinder. *Energies*, 14(17), 5582. <https://www.mdpi.com/1996-1073/14/17/5582>

Hooper, M. L., & McKeon, B. J. (2021). A representative driven system to interrogate passive dynamics of an airfoil in the wake of a cylinder. In *14th International Symposium on Particle Image Velocimetry*, 1(1). <https://scholar.archive.org/work/qru6vcoszbedhfbvsawwf6mci/access/wayback/https://ispirv21.library.iit.edu/index.php/ISPIV/article/download/167/170>

Kim, D. H., Chang, J. W., & Chung, J. (2011). Low-Reynolds-number effect on aerodynamic characteristics of a NACA 0012 airfoil. *Journal of Aircraft*, 48(4), 1212-1215. <https://arc.aiaa.org/doi/pdf/10.2514/1.C031223>

Gorakkh, M. H. G. & Khoshnevis, A. B. (2025). Investigating the pressure distribution of an airfoil with a cylindrical body. *World Journal of Environmental Research*, 15(2), 132-145. <https://doi.org/10.18844/wjer.v15i2.9918>

Lefebvre, J. N. (2021). *Cylinder-Airfoil Interactions and the Effect on Airfoil Performance* (Doctoral dissertation, University of Maryland, College Park). <https://search.proquest.com/openview/fe8d320eda3bae8142fa64bfc61c75f9/1?pq-origsite=gscholar&cbl=18750&diss=y>

Lefebvre, J. N., & Jones, A. R. (2019). Experimental investigation of airfoil performance in the wake of a circular cylinder. *AIAA Journal*, 57(7), 2808-2818. <https://arc.aiaa.org/doi/abs/10.2514/1.J057468>

Liao, Q., Dong, G. J., & Lu, X. Y. (2004). Vortex formation and force characteristics of a foil in the wake of a circular cylinder. *Journal of fluids and structures*, 19(4), 491-510. <https://www.sciencedirect.com/science/article/pii/S0889974604000441>

Mittal, R., & Balachandar, S. (1995). Effect of three-dimensionality on the lift and drag of nominally two-dimensional cylinders. *Physics of Fluids*, 7(8), 1841-1865. <https://pubs.aip.org/aip/pof/article-abstract/7/8/1841/259460>

Nadery, A., Bahrami, H., Najafi, A., Ghassemi, H., Aminzadeh, M., & He, G. (2025). Numerical investigation of toroidal propeller: hydrodynamic and hydroacoustic study. *Ships and Offshore Structures*, 1-16. <https://www.tandfonline.com/doi/abs/10.1080/17445302.2025.2477771>

Rad, M. P., & Khoshnevis, A. B. (2023). Experimental investigation of flow structure over pitching airfoil in the wake of circular cylinder. *Ocean Engineering*, 284, 115103. <https://www.sciencedirect.com/science/article/pii/S0029801823014877>

Takagi, Y., Fujisawa, N., Nakano, T., & Nashimoto, A. (2006). Cylinder wake influence on the tonal noise and aerodynamic characteristics of a NACA0018 airfoil. *Journal of Sound and Vibration*, 297(3-5), 563-577. <https://www.sciencedirect.com/science/article/pii/S0022460X06003117>

Wang, T., Feng, L. H., Cao, Y. T., & Wang, J. J. (2024). Airfoil response to periodic vertical and longitudinal gusts. *Journal of Fluid Mechanics*, 979, A35. <https://www.cambridge.org/core/journals/journal-of-fluid-mechanics/article/airfoil-response-to-periodic-vertical-and-longitudinal-gusts/EE490381B8A319D348820E1A447F57C8>

Yang, Y., Li, P., Li, C., Wang, Y., Liu, Y., Liu, C., & Arcondoulis, E. J. (2025). Impact of vortex interference on airfoil tonal noise emission. *Physics of Fluids*, 37(4). <https://pubs.aip.org/aip/pof/article/37/4/045143/3343168>

Zhao, Y., Li, M., & Yang, Y. (2025). Insights into the aerodynamic response of a harmonic oscillating airfoil in various turbulent flows. *Communications Engineering*, 4(1), 170. <https://www.nature.com/articles/s44172-025-00503-5>